High-intensity laser-induced electron acceleration in vacuum

J. X. Wang,[1] Y. K. Ho,[1,2,*] L. Feng,[1] Q. Kong,[1] P. X. Wang,[1] Z. S. Yuan,[1] and W. Scheid[3]
[1]*Institute of Modern Physics, Fudan University, Shanghai 200433, China*
[2]*CCAST (World Laboratory), P.O. Box, Beijing 100080, China*
[3]*Institute for Theoretical Physics, Justus-Liebig-University Giessen, D35392 Giessen, Germany*
(Received 17 May 1999)

In this paper, an approximate pulsed-laser-beam solution of Maxwell's equation in vacuum is derived. Then with the numerical simulation method, electron acceleration induced by high-intensity $[Q_0=eE_0/(m_e\omega c)=3]$ lasers is discussed in connection with the recent experiment of Malka *et al.* It is found that the maximum energy gain and the relationship between the final energy and the scattering angle can be well reproduced, but the polarization effect of electron-laser interactions is not very prominent. These results show that the ponderomotive potential model is still applicable, which means that the stimulated Compton scattering is the main fundamental mechanism responsible for the electron acceleration at this laser intensity.
[S1063-651X(99)09012-1]

PACS number(s): 41.75.Fr, 42.50.Vk, 42.50.Hz

I. INTRODUCTION

More than ten years of work in the past led to the development of the chirped-pulse amplification (CPA) [1] which has made multiterawatt compact short-pulse lasers readily available in laboratories. To date, the focused laser intensities can reach as high as $I\lambda^2\sim10^{19}$ (W/cm^2) μm^2 [2], where I and λ are the focused laser intensity and wavelength in units of W/cm^2 and μm. At this intensity, the electron quivering energy $V_{\rm osc}=(\sqrt{1+Q_0^2/2}-1)m_ec^2\approx0.6$ MeV is already larger than the electron rest energy. $Q_0=eE_0/(m_e\omega c)$ is a dimensionless parameter measuring the field intensity, E_0 is the magnitude of the laser field at focus, m_e the electron rest mass, ω_0 the laser angular frequency, $-e$ the electron charge, and c the light speed in vacuum. By using $I\lambda^2=1.37\times10^{18}Q_0^2$(W/cm^2) μm^2, we have $Q_0\approx3$. According to our previous findings [3], this corresponds to the transition region $(0.1<Q_0<10)$ from ordinary Compton scattering to nonlinear Compton scattering (NLCS) [4] underlying the free-electron–laser interaction. NLCS is characterized by a process in which two or more photons are absorbed simultaneously by the free electron accompanied with the emission of a single higher-frequency photon. Recently electrons accelerated to MeV energy in vacuum by intense lasers with $Q_0=3$ [5] were experimentally observed. It should be mentioned that, earlier, electrons were accelerated to a fraction of eV [6] or a few keV [7] at low intensity and 100 keV [8] for electrons initially at rest at higher intensity. If we claim that NLCS is responsible for most of the energy transfer between free electrons and lasers when $Q_0>10$, then comes the question of what fundamental mechanism can account for the large electron energy gain when interacting with lasers with $Q_0<10$. In this paper, we will show that the stimulated Compton scattering (SCS) [9] is the mechanism we are seeking, which means that after absorbing a photon from the laser field the free electron tends to emit one photon which is of the same frequency as another passing photon. The reasons are summarized as follows. First, from a classical viewpoint such a large energy change of electrons can only occur in the pulsed laser fields because when a continuous laser beam with $Q_0=3$, is applied, only hundreds of eV energy can be obtained by our previous calculation. Second, from a quantum viewpoint, SCS can only result in momentum, not energy, transfer between the electrons and a continuous laser field, because a continuous laser field can be Fourier expanded but all components are plane waves traveling in slightly different directions with the same frequency. For a pulsed laser beam it is quite different, because the corresponding Fourier-expanded components not only can be of different directions but also of different frequencies, and SCS can lead to photon redistribution in different modes of laser fields.

Another aim of this paper is to study in detail the characteristics of electron scattering by a pulsed laser beam based on Malka's experiment since its theoretical interpretation caused much discussions [10]. The controversy mainly focuses on the field equations they used, which do not satisfy the free-space Maxwell equations. To overcome the problem, we have generalized our previous field equations, which were valid for continuous laser beams to pulsed laser beams. They satisfy Maxwell's equations approximately. By including all the field components, we put our description of an electron–pulsed-laser interaction on more solid ground.

In the following, the pulsed-laser field solution will be present first. Then our computation model is described. Next, by numerical simulation, electron-scattering characteristics in the pulsed-laser beam are discussed in detail based upon Malka's experiment. The comparison with the description of the ponderomotive potential model is also given. Finally a summary of the conclusions drawn in this paper is given.

II. PULSED-LASER-BEAM SOLUTION OF MAXWELL'S EQUATIONS

In the following discussion, the Lorentz gauge is used, i.e., the scale and vector potentials $\Phi,\vec{A}$ satisfy the relationship

*Author to whom correspondence should be addressed. Address correspondence to Institute of Modern Physics, Fudan University, Shanghai 200433, China. FAX:+86-21-65104949. Electronic address; hoyk@fudan.ac.cn

$$\vec{\nabla}\cdot\vec{A}+\frac{1}{c^2}\frac{\partial\Phi}{\partial t}=0. \tag{1}$$

The electric and magnetic components can be obtained by using

$$\vec{E}=-\frac{\partial\vec{A}}{\partial t}-\vec{\nabla}\Phi \tag{2}$$

$$\vec{B}=\vec{\nabla}\times\vec{A}. \tag{3}$$

For a linearly polarized pulsed-laser beam, we assume $\vec{A}$ and Φ to be of the following form:

$$\vec{A}=g(\eta)\Lambda(x,y,z)e^{i\eta}\hat{e}_x$$

$$=g(\eta)A\hat{e}_x, \tag{4}$$

$$\Phi=g(\eta)\Gamma(x,y,z)e^{i\eta}, \tag{5}$$

in which $\eta=\omega t-kz,\hat{e}_x$ is the unit vector along the x axis representing the laser polarization direction, and $g(\eta)=e^{-}(\eta/\omega\tau)^2$ is the form factor of the laser pulse with τ the pulse length. Substituting the above equations in Eq. (1), it can be found that

$$\Gamma(x,y,z)=\frac{ic^2g(\eta)}{\omega\left(1-i\dfrac{g'(\eta)}{g(\eta)}\right)}\frac{\partial\Lambda}{\partial x}e^{i\eta}, \tag{6}$$

where $g'(\eta)=dg(\eta)/d\eta$. Hence if $\vec{A}$ is obtained, $\vec{E}$ and $\vec{B}$ can be easily obtained by using Eqs. (2) and (3). As is well known, $\vec{A}$ meets the following wave equation:

$$\nabla^2\vec{A}-\frac{1}{c^2}\frac{\partial^2}{\partial t^2}\vec{A}=0. \tag{7}$$

Replacing $\vec{A}$ with Eq. (4), we have

$$\left(\frac{\partial^2}{\partial x^2}+\frac{\partial^2}{\partial y^2}\right)\Lambda+\frac{\partial^2\Lambda}{\partial x^2}-2ik\frac{\partial\Lambda}{\partial y}+2k\frac{g'(\eta)}{g(\eta)}\frac{\partial\Lambda}{\partial z}=0. \tag{8}$$

It is almost impossible to find an exact analytical solution to the above equations. The more realistic step is to find an approximate one. For this reason, we introduce three dimensionless parameters to describe the characteristic lengths of the laser beam in free space,

$$x=w_0\xi,\quad y=w_0\zeta,\quad z=kw_0^2\varsigma, \tag{9}$$

in which kw_0^2 is proportional to the Rayleigh range length $z_R(=kw_0^2/2)$ of the laser beam. Using ξ,ζ,ς instead of x,y,z, Eq. (8) is rewritten as

$$\left(\frac{\partial^2}{\partial\xi^2}+\frac{\partial^2}{\partial\zeta^2}\right)\Lambda-2i\frac{\partial\Lambda}{\partial\varsigma}=\frac{4\eta}{(\omega\tau)^2}\frac{\partial\Lambda}{\partial\varsigma}-s^2\frac{\partial^2\Lambda}{\partial\varsigma^2}, \tag{10}$$

where $s=1/(kw_0)$ is a small factor, which can be used to expand Λ Considering $1/(\omega\tau)\ll 1/(kw_0)$ and making use of

$$\Lambda=\Lambda_0+s^2\Lambda_2+s^4\Lambda_4+\cdots, \tag{11}$$

we have

$$\left(\frac{\partial^2}{\partial\xi^2}+\frac{\partial^2}{\partial\zeta^2}-2i\frac{\partial}{\partial\zeta}\right)\Lambda_0=0,$$

$$\left(\frac{\partial^2}{\partial\xi^2}+\frac{\partial^2}{\partial\zeta^2}-2i\frac{\partial}{\partial\zeta}\right)\Lambda_2=\left[-\frac{\partial}{\partial\varsigma}+4\eta\left(\frac{kw_0^2}{w\tau}\right)^2\right]\Lambda_0, \tag{12}$$

$$\vdots$$

to zero order and second order, etc., of s. The equation satisfied by Λ_0 is the same as those obtained by Davis [11] and its fundamental-mode solution is known to be the Hermite-Gaussian (0,0) mode laser beams [12].

After Λ is known, $\vec{E}$ and $\vec{B}$ are solved as follows by using Eqs. (2) and (6):

$$\vec{E}=-\frac{\partial\vec{A}}{\partial t}-\vec{\nabla}\Phi$$

$$=\hat{e}_x\left[-\frac{i\omega}{1+i\dfrac{2\eta}{(\omega\tau)^2}}\frac{\partial^2A}{\partial\xi^2}s^2+\omega\frac{2\eta}{(\omega\tau)^2}A-i\omega A\right]g(\eta)$$

$$+\hat{e}_y\frac{i\omega}{1+i\dfrac{2\eta}{(\omega\tau)^2}}\frac{\partial^2A}{\partial\xi\partial\zeta}s^2-\hat{e}_z\left[i\frac{s}{g(\eta)}\frac{\partial}{\partial\eta}\left(\frac{g(\eta)}{1+i\dfrac{2\eta}{(\omega\tau)^2}}\right)\right.$$

$$\left.+\frac{s}{1+i\dfrac{2\eta}{(\omega\tau)^2}}+s^3t\right]\frac{\partial A}{\partial\xi}\omega g(\eta). \tag{13}$$

By preserving factors exact to order s and using the Hermite-Gaussian (0,0) mode laser beam, we can have

$$\vec{E}=-\hat{e}_x[i\omega Ag(\eta)]+\hat{e}_z\left(\frac{\partial A}{\partial\xi}g(\eta)s\right), \tag{14}$$

in which

$$A=E_0\frac{1}{w(\varsigma)}e^{-\xi^2+\zeta^2/w(z)^2}e^{-i\{\eta-\varphi(\varsigma)-\varphi_0-[(\xi^2+\zeta^2)/2R(\varsigma)]\}}, \tag{15}$$

with

$$w(\varsigma)=w_0[1+(2\varsigma)^2]^{1/2}, \tag{16}$$

$$R(\varsigma)=z\left[1+\left(\frac{1}{2\varsigma}\right)^2\right], \tag{17}$$

$$\varphi(\varsigma)=\tan^{-1}\left(\frac{1}{2\varsigma}\right). \tag{18}$$

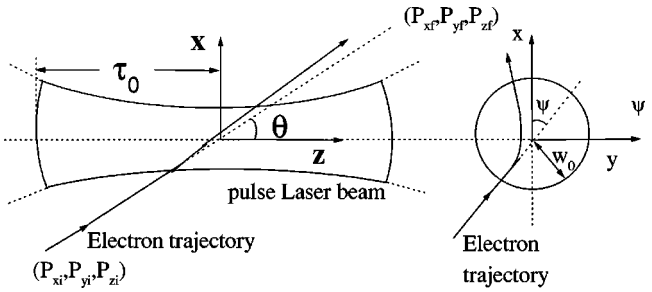

FIG. 1. Schematic geometry of electron scattering by a pulse-laser beam. The pulse laser propagates along the z axis. w_0 is the beam width at the waist. τ_0 is the pulse length. Without losing generality, we assume electrons come from the minus-x side directed to the beam center. $(\gamma_i, P_{xi}, P_{yi}=0, P_{zi})$ denote the incoming energy and momentum of the electron and $(\gamma_f, P_{xf}, P_{yf}, P_{zf})$ that of the outgoing state. γ is the Lorentz factor and b_0 is the impact parameter. $\theta=\tan^{-1}(P_{xi}/P_{zi})$ is the electron incident angle, and $\psi=\tan^{-1}(P_{yi}/P_{xi})$ is the azimuthal angle.

Similarly,

$$\vec{B}=\vec{\nabla}\times\vec{A}\approx\hat{e}_y[-ikAg(\eta)]+\hat{e}_z\left(\frac{\partial A}{\partial\xi}g(\eta)s\right). \quad (19)$$

III. COMPUTATION MODEL

Once we have obtained the mathematical expression of the pulse-laser beams, the electron dynamics can be studied by solving the following relativistic Lorentz equation:

$$\frac{d\vec{P}}{dt}=-e(\vec{E}+\vec{V}\times\vec{B}), \quad (20)$$

in which $\vec{P}=m_e\gamma\vec{V}$ is the electron momentum with $\vec{V}$ the speed and γ the Lorentz factor. Because of the complexity of the laser fields, the above nonlinear equation can only be solved numerically. For this purpose, the fourth-order Runge-Kutta together with Richardson's first-order extrapolation procedure [13] were used to acquire one-order higher accuracy. The step size is adjusted automatically with a minimal time step $0.01T/2\pi$, with T the laser oscillation period, which is sufficient for the fields considered in this paper.

Figure 1 shows the configuration of free-electron–pulse-laser interaction. Based upon Malka's experiment, lasers with $I=10^{19}$ W/cm^2, $\lambda=1.056$ and $\tau=300$ fs, $w_0=10$ μm are used. The electron is incident with a crossing angle $\theta=10°$ to the laser propagation direction and with $|\vec{V}|=0.1c$, corresponding to an incident kinetic energy 2.5 keV. The standard initial time t_0 is chosen so as to let the electron reach the focus center $(x=y=z=0)$ at $t=0$, i.e., $t_0=-r_0/|\vec{V}_0|$, where r_0 is the initial distance of the electron from the focus center and $|\vec{V}_0|$ is the initial velocity. To express the fact that the electron may sample different parts of the laser beam, a delay time Δt relative to t_0 is introduced. It is negative when the electron meets the leading edge of the laser beam and positive when the electron meets the trailing edge.

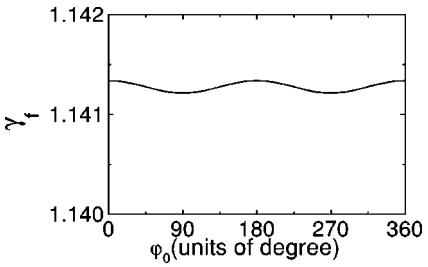

FIG. 2. Influence of the initial phase φ_0 upon the electron final energy (measured by the Lorentz factor γ_f in units of m_ec^2). The electron with $|\vec{V}|=0.1c$ and $\Delta t=0$ is injected upon the laser of $Q_0=3$, $\omega\tau_0=535$, and $kw_0=60$ with a crossing angle $\theta=10^0$ and an azimuthal angle $\psi=0$. These parameters are used in all the following figures unless otherwise mentioned. The difference between the maximum and minimum value of γ_f is 64 eV.

The concrete results will be presented and discussed in the next section.

IV. NUMERICAL RESULTS AND DISCUSSIONS

As found in our previous research, because of the nonlinearity of Eq. (16), the electron scattering is sensitive to the initial phase φ_0 especially when $Q_0>10$. But in the case $Q_0=3$, it can be easily found from Fig. 2 that the electron final energy changes very little against φ_0 (the difference between the maximum and minimum final energy is only tens of eV). Thus in the following calculation, it is reasonable to omit the influence of φ_0, which is set to a fixed value $\varphi_0=0$.

A. Polarization effect

Besides field equations, the polarization effect is another much discussed point following Malka's experiment since it is closely related to the validity of the ponderomotive potential model. To probe this effect, we presented in Fig. 3 the relationship between the azimuthal angle ψ and the electron final energy $m_ec^2\gamma_f$; the electron initial motion is directed to the beam center with a fixed crossing angle θ One can see this even though γ_f reaches minimum when the electron is injected vertical to the laser polarization plane ($\psi=90°,270°$) and maximum when injected in the polarization plane ($\psi=0°,180°$). Their difference (of 25 eV) is not so large as to disrupt the axis symmetry of the electron scattering. This result is consistent with that presented in the comments by MacDonald and Mora [10]. The nearly isotropic

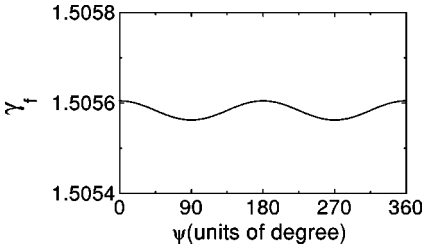

FIG. 3. Demonstration of the polarization effect upon the electron final energy. $\varphi_0=0$, which is used in all the following figures. The difference between the maximum and minimum value of γ_f is 25 eV.

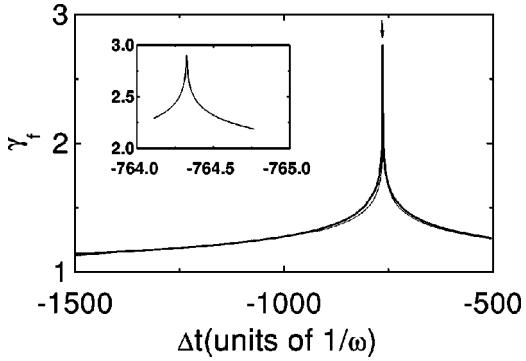

FIG. 4. Variation of the electron final energy against the delay time $\omega\Delta t$. The solid line is calculated by using realistic fields and the dotted line by using the ponderomotive potential model. The inset is the enlargement of the part denoted by the arrow.

scattering with ψ implies that the ponderomotive potential model to some extent might be a valid description of free-electron–laser interaction. To be more decisive, we will compare the results obtained using the two methods in the next part.

B. Maximum energy transfer

The ponderomotive potential [14] can be written as

$$V_{\mathrm{pon}}=\left(\sqrt{1+\frac{Q^2}{2}}-1\right)m_e c^2, \tag{21}$$

where

$$Q=Q_0 g(\eta)\frac{w_0}{w(z)}e^{-(x^2+y^2)/w(z)^2}. \tag{22}$$

Similar to Eq. (20), the electron motion in this potential can be acquired by solving the following relativistic Newtonian equation:

$$\frac{d\vec{P}}{dt}=-\nabla V_{\mathrm{pon}} \tag{23}$$

Figure 4 shows the relationship between γ_f and Δt. It is interesting to note that the final energy predicted by the descriptions of realistic laser fields and the ponderomotive potential model coincides very well. We have known that the ponderomotive potential describes the electron oscillation in a laser field. The oscillation was argued [6] to be the result of a kind of stimulated scattering process in which photons scatter from one occupied laser mode to another, viz., SCS, resulting in both momentum and energy transfer to the electron. Thus the ponderomotive potential description embodies the contribution from SCS classically. From this argument, it is safe to say that the SCS can be regarded as the fundamental mechanisms underlying the large energy gain of the electron since the results obtained from the ponderomotive potential agree very well with those obtained using the realistic fields. The maximum energy in Fig. 4 is shown to be 0.9 MeV, which is consistent with the measured value [5].

By close observation, it can be found that when $\Delta t \ll 0$, the electron is affected only by a very weak laser field and

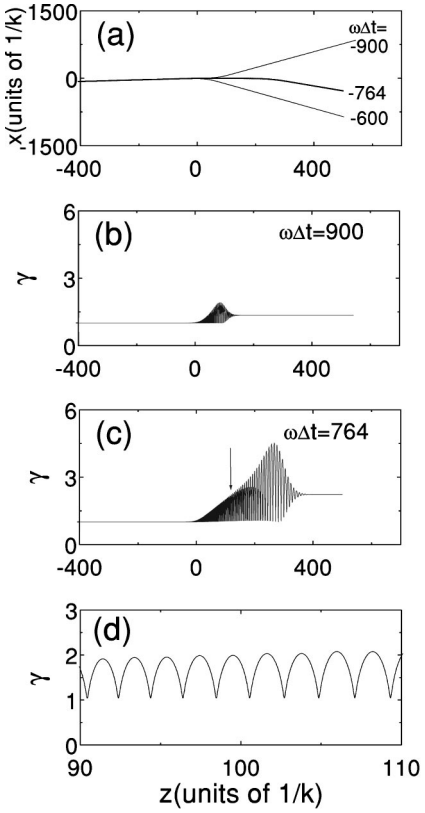

FIG. 5. Single electron dynamics with different delay time $\omega\Delta t$. (a) Electron trajectories with $\omega\Delta t=-900,-764$, and -600. (b) and (c) show the variation of electron energy with $\omega\Delta t=-900$ and -764, respectively. (d) is the enlargement of the part denoted by the arrow shown in (c).

can easily go through the laser beam. As Δt increases near zero, the electron will encounter more and more intense fields until it reaches a point where it is reflected by the central strong field region. At such a critical turning point, the electron will surf along the laser field for a much longer time than in other cases, leading to a larger energy gain. Thus in Fig. 4 the maximum value appears near the critical turning point. The above process is clearly shown in Fig. 5 for different delay time Δt.

Another interesting phenomenon of the electron scattering is that the interaction time is influenced very much by the beam width w_0. The larger the beam width is, the longer the electron will stay in the laser field before being scattered out. Hence, near the turning point, the electron will gain more energy since it surfs along the laser pulse for a longer time. This is well demonstrated in Fig. 6, in which a laser pulse with beam width $w_0=34$ μm ($kw_0=200$) is used. The electron final energy is found to be 1.3 MeV, larger than 0.9 MeV when the $w_0=10$ μm laser is applied. Of course, this result is valid only when the pulse length is relatively long, because when too short a pulse is used, the electron will soon slide to the negative-gradient part of the lasers and begin to lose energy. This is truly an effect for pulse lasers, quite different from what happens in the continuous ones. In a continuous laser beam with narrow width, namely greater transverse space gradient of field intensity, we found in our previous work [3] larger final electron energy. The reason for this difference lies in the fact that the longitudinal field gra-

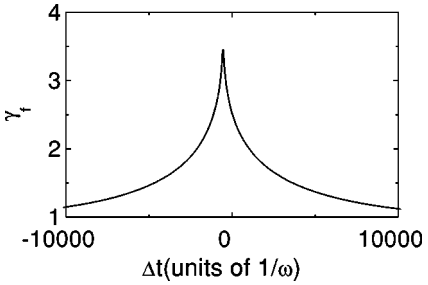

FIG. 6. The same as in Fig. 4 but for lasers with beam width $kw_0=200$.

dient in pulse-laser scattering plays the most important role in electron acceleration, while in continuous laser scattering only the transverse field gradient plays such a role.

It is known that the field spacial gradient is an overall effect of all the field components and that the transverse electric field plays the most important role in the electron dynamics. In order to see the relative importance of other field components, we give two calculations below. First, the delay time is chosen to be far away from the critical turning point, as discussed above, and we find that both the transverse magnetic field and the longitudinal electric field are not important to the electron final energy and can almost be neglected. This may be because under such circumstances the electron interacts with the laser beam very briefly. Second, the delay time is chosen to be near the critical turning point, where the electron will surf along the pulse beam for a much longer time. Things begin to change. For example, when using $\omega\Delta t=-764$, we can have the final electron energy to be 0.59 MeV with no longitudinal electric-field component included in the description of the laser beams and 0.26 MeV with no transverse magnetic one. When all the field components are considered, the corresponding value is 0.63 MeV. From these data, we can say that the transverse magnetic-field component makes a greater contribution to the electron final energy than the longitudinal electric one does. The difference can be partly explained from the facts that the Lorentz force $\vec{V}\times\vec{B}$ is one order of magnitude smaller than E_x with the concerned electron energy while E_z is nearly two orders of magnitude smaller than E_x, as shown in Eq. (13).

C. $\gamma_f-\theta_f$ relationship

In a field with the vector potential of the form

$$\vec{A}=A_0[\hat{e}_x\delta\cos(\eta)+\hat{e}_y\sqrt{1-\delta^2}\sin(\eta)]f(\eta), \qquad (24)$$

where A_0 is the amplitude, δ gives the degree of ellipticity, and $f(\eta)$ is an arbitrary pulse shape function, the following relationship between the scattering angle θ_f and final energy γ_f in units of m_ec^2 is an exact motion integral [15–17]:

$$\tan\theta_f=\frac{\sqrt{\vec{P}^2_{\text{tran }0}+2(\gamma_0-P_{z0})(\gamma_0-\gamma_f)}}{P_{z0}+\gamma_0-\gamma_f}, \qquad (25)$$

in which $\vec{P}_{\text{tran0}}$ and P_{z0} are the electron initial momentum in the transverse and longitudinal direction, respectively, and γ_0 is the initial electron energy. It may then be asked, what about the case when a realistic laser beam with a transverse

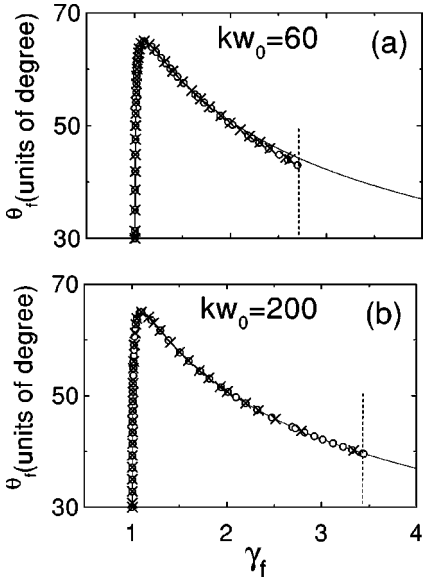

FIG. 7. θ_f-γ_f relationship obtained with different methods: using Eq. (25) (solid line), calculating through realistic fields (open circle ○) and ponderomotive potential model (cross ×). (a) is for $kw_0=60$ and (b) is for $kw_0=200$. The maximum final energy of the electron is denoted by vertical dotted lines in (a) and (b).

space gradient is used, such as the lasers used in this paper? Figure 7(a) presents the variation of the scattering angle θ_f against the electron final energy calculated by Eq. (20) and Eq. (25). It is apparent that only in the high-energy region does Eq. (25) begin to deviate from the results obtained using realistic fields. The deviation depends strongly on the transverse field gradient because when lasers with lower transverse field gradient, e.g., $kw_0=200$, are used, the relationship Eq. (25) holds up very well as can be easily seen from Fig. 7(b). Thus Eq. (25) can be regarded as a motion integral of high precision so long as the laser beam width is not too small. A possible application of such scattering is to use it as a very effective electron injector of low-energy emittance in laser acceleration as done by Moore [18].

As stated in Sec. III (B), the ponderomotive potential provides a good description of the electron energy gained. By calculating the $\gamma_f-\theta_f$ relationship from this model, we showed its validity by noting the consistency with the results of Eq. (23) as presented in Fig. 7. It should be mentioned that the maximum electron energy gain cannot be obtained from Eq. (25). It was obtained by numerical simulation of electron motion. Summarizing the results, the maximum energy of the scattered electron 0.9 MeV corresponds to a scattering angle 42° when $|\vec{V}|=0.1c$, which is close to the experiment data 39°. The difference may be attributed to the estimated laser beam width being low since the laser beam with a higher transverse field gradient will lead to a smaller scattering angle according to the variation trend shown in Fig. 7.

V. CONCLUSIONS

Our conclusions in this paper can be summarized as follows.

(i) By using our pulse-laser field equations, the maximum energy and $\gamma_f-\theta_f$ relationship obtained in Malka's experiment have been reproduced [5].

(ii) No obvious polarization effect of the electron scattering was found at $Q_0=3$. The ponderomotive potential provides a good approximation to the real laser field. The large energy transfer of MeV magnitude can be attributed to SCS.

(iii) When the pulse length is not too short, a wider beam width will yield electron higher maximum energy gain for the same Q_0. This prediction hopefully will soon be confirmed by experimental tests.

As Q_0 is increased to be larger than 10, NLCS, whose contribution is proportional to Q_0^2, begins to play a dominant role in electron scattering. Because the contribution of SCS is proportional to Q_0, it will be a very interesting job to compare the two effects. Moreover, when $Q_0>10$, the polarization effect will start to play its role. We plan to investigate these in detail.

ACKNOWLEDGMENTS

The authors would like to thank Professor Z. M. Fu for a careful reading of this manuscript and enlightening discussion. This work was supported partly by the National Natural Science Foundation of China under Contract No. 10684001, the National High-Tech ICP Committee in China, and the Engineering-Physics Research Institute Foundation of China under Contract No. 9838.

[1] D. Strickland and G. Mourou, Opt. Commun. **56**, 219 (1985).
[2] N. Blanchot *et al.*, Opt. Lett. **20**, 395 (1995); G. Rouyer *et al.*, *ibid.* **13**, 55 (1995).
[3] Y.K. Ho, J.X. Wang, L. Feng, W. Scheid, and H. Hora, Phys. Lett. A **220**, 189 (1996); J.X. Wang, Y.K. Ho, and W. Scheid, *ibid.* **231**, 139 (1997); *ibid.* **234**, 415 (1997).
[4] K.T. McDonald, in *Laser Acceleration of Particles*, edited by Chan Joshi and Thomas Katsouleas (AIP, New York, 1985), no. 130, p. 23; K.T. McDonald, P. Chen, J.E. Spencer, and R.B. Palmer, in *Proceedings of the Workshop on Beam-beam and Beam-radiation Interactions—High Intensity and Nonlinear Effects* (World Scientific, Singapore, 1992), p. 127; C. Bula *et al.*, Phys. Rev. Lett. **76**, 3116 (1996).
[5] G. Malka, E. Lefebvre, and J.L. Miquel, Phys. Rev. Lett. **78**, 3314 (1997).
[6] Ph. Bucksbaum, M. Bashkanski, and T.J. McIlrath, Phys. Rev. Lett. **58**, 349 (1987).
[7] P. Monot *et al.*, Phys. Rev. Lett. **70**, 1232 (1993).
[8] C.I. Moore, J.P. Knauer, and D.D. Meyerhofer, Phys. Rev. Lett. **74**, 2439 (1995); D.D. Meyerhofer, J.D. Knauer, S.J. Naught, and C.I. Moore, J. Opt. Soc. Am. B **13**, 113 (1996).
[9] L.S. Bartell, H.B. Thompson, and P.R. Roskos, Phys. Rev. Lett. **14**, 851 (1965).
[10] K.T. MacDonald, Phys. Rev. Lett. **80**, 1350 (1998); P. Mora and B. Quesnel, *ibid.* **80**, 1351 (1998); E. Lefebvre, G. Malka, and J.L. Miquel, *ibid.* **80**, 1352 (1998).
[11] L.W. Davis, Phys. Rev. A **19**, 1177 (1979).
[12] O. Svelto, and D.C. Hanna, *Principles of Lasers*, 3rd ed. (Plenum Press, New York, 1989).
[13] M.L. James, G.M. Smith, and J.C. Wolfford, *Applied Numerical Method for Digital Computation*, 3rd ed. (Harper & Row, New York, 1985).
[14] T.W.B. Kibble, Phys. Rev. **150**, 1060 (1966); Phys. Rev. Lett. **16**, 1054 (1966).
[15] F.V. Hartemann *et al.*, Phys. Rev. E **51**, 4833 (1995).
[16] Y.I. Salamin and F.H.M. Faisal, Phys. Rev. A **55**, 3678 (1997).
[17] B. Quesnel and P. Mora, Phys. Rev. E **58**, 3719 (1998).
[18] C.I. Moore *et al.*, Phys. Rev. Lett. **82**, 1688 (1999).